

Evaluation of fiber dispersion of PVA-ECC

Y. Y. Kim¹, B. Y. Lee² and J. K. Kim²

Summary

The fiber dispersion performance in fiber-reinforced cementitious composites is a crucial factor with respect to achieving desired mechanical performance. However, evaluation of the fiber dispersion performance in the composite PVA-ECC (Polyvinyl alcohol-Engineered Cementitious Composite) is extremely challenging because of the low contrast of PVA fibers with the cement-based matrix. In the present work, an enhanced image processing technique including more detailed classification of types of fibers and adaptation of a morphological reconstruction, the fiber detection performance is enhanced. Test results using artificial and real fiber images showed that a distribution coefficient α_f , referred to as the fiber dispersion coefficient was calculated reasonably and the fiber detection performance was enhanced.

Introduction

Synthetic fibers have been used to improve the toughness of quasi-brittle cement-based materials such as concrete and mortar[1]. Recently developed ultra-ductile engineered cementitious composite (ECC) is an example of this approach[2-3]. ECC is a micromechanically designed cementitious composite that exhibits extreme tensile strain capacity (typically more than 2%) while requiring only a moderate amount of fibers (typically less than 2% in a volume fraction). Since the fibers can bridge micro-cracks, the dispersion of fibers strongly influences the resulting mechanical performance of the composite.

Transmission X-ray photography, which is generally applied to steel fiber-reinforced composites, is the most popular method of evaluating the degree of fiber dispersion, i.e., how steel fibers are homogeneously dispersed in the composite. The evaluation of organic fiber dispersion, however, has seen little attention. The key step in performing an evaluation of organic fiber dispersion is the fiber detection, since the contrast of organic fibers with cementitious materials is too low to allow detection in the composite. To overcome this, a fluorescence technique has been employed specifically to detect polyvinyl alcohol (PVA) fibers.

Torigoe et al.[4] suggested a new evaluation method for PVA fiber dispersion. After capturing the fluorescence image with a Charged Couple Device (CCD) camera through a microscope, the image is divided into small units of appropriate pixel size. The degree of fiber dispersion is then calculated based on the deviation from

¹Dept. of Civil Engineering, Chungnam National University, Korea

²Dept. of Civil & Environmental Engineering, Korea Advanced Institute Science and Technology, Korea

the average number of fibers in a unit, which is obtained by a rigorous process of directly counting the fibers point by point. In addition, the distribution coefficient, which represents the degree of fiber dispersion, significantly depends on the size of the unit.

In the present work, the authors describe a new image processing procedure to eliminate both rigorous, manual fiber-counting processes and the undesirable impact of the unit size on the distribution coefficient. In the development of the suggested method, the fiber detection performance was enhanced by employing the morphological reconstruction and watershed segmentation technique.

Evaluation of fiber dispersion

The first step for evaluation of fiber dispersion is preparation and treatment of the specimen. PVA-ECC specimens were produced on the basis of micromechanical principles[1] and then cured in water at 20 ± 3 °C for 28 days. Specimens were cut with a diamond saw to obtain samples for fiber dispersion evaluation. Each sample, a rectangular block with a size of $13 \times 36 \times 20$ mm, was polished to create a smooth surface of the exposed cross-section.

The second step is image acquisition. The polished surface was then photographed using image acquisition equipment, which was composed of a fluorescence microscope (Olympus, BX51), a CCD camera, and image processing software. To obtain a digital image, the sample surface was first illuminated by a mercury lamp, followed by capture of a fluorescent image using a CCD digital camera through a GFP filter under $4 \times$ magnification.

The third and final step are automatic detection of fibers in a cross-sectional fluorescence image and mathematical treatment of the data obtained from the previous step. The degree of fiber dispersion is then quantitatively evaluated based on the calculation of a distribution coefficient α_f , referred to as the fiber dispersion coefficient, as expressed by equation (1) as follows[5].

$$\alpha_f = \exp \left[-\sqrt{\frac{\sum (x_i - 1)^2}{n}} \right] \quad (1)$$

where n is the total number of fibers on the image, and x_i denotes the number of fibers in the i -th unit, which is a square portion allocated to the i -th fiber on the assumption that the fiber dispersion is perfectly homogeneous. The fiber dispersion coefficient α_f is automatically calculated via the following algorithm (prototype algorithm): (1) Convert the RGB image to a grayscale image, (2) Convert the grayscale image to a binary image based on a set threshold, (3) Divide the binary image into units, i.e., equivalent squares, of which the total number equals the number of fibers (n), (4) Obtain the coordinate data for the centroid of each fiber image,

and (5) Count the number of fibers (x_i) located in each unit.

Image processing technique for enhancing fiber-detection performance

In order to obtain a more accurate dispersion coefficient, an additional process was developed and inserted between step (2) and step (3) (described in the previous section). The added process basically consists of two parts: one is for categorizing fiber images into five types, and the other is for dividing aggregate fiber images into individual fiber images. Fig. 2 shows the procedure of the enhanced detection algorithm. The number of fibers detected by binarization technique[6] is compared with that detected by watershed segmentation technique. If the number of fibers is same, the fiber image is classified as Type 1w, otherwise, four types (Type 1, 2, 3 and 4) by a classifier. Fig. 3 shows typical fiber image according to fiber image types. Type 1 represents single fiber images whose cross-sectional shape is roughly circular, however, the number of fibers detected is more than two by watershed segmentation technique due to irregularity of brightness of image. Type 2 mainly correspond to aggregate fibers incorrectly detected as a single fiber. Type 2 is detected correctly by watershed segmentation technique. Type 3 represents the aggregate fiber images lined up in succession and oriented at diverse angles to the surface plane, therefore incorrectly detected as a single fiber. To detect correctly Type 3, watershed segmentation technique is applied after morphological reconstruction of fiber image. This process is for minimization of over-segmentation. Type 4 includes images of single fibers oriented at roughly right angles to the surface plane.

To classify the fiber images, artificial neural network(ANN) is constructed. Features which are used as input of classifier are extracted considering invariant to image translation, scaling and rotation. Those are solidity(F_s : the division of an object's area by that of the object's convex hull), packing density(F_c : the division of an object's area by that of the object's circumscribed circle), unit perimeter(F_p : the division of an object's perimeter by the object's area), unit length(F_l : the division of an object's major length by the object's area), relative length(F_{lre} : the division of an object's major length by average length of whole fiber images). The structure of ANN is determined on the basis of 10-fold cross validation. One hidden layer is used. The hyperbolic tangent sigmoid function and linear function are used as a transfer function on each neuron of hidden layer and output layer. The Levenberg-Marquardt algorithm with weight decay[7] is adopted as a learning algorithm in order to prevent over-fitting. The optimum network architecture is accordingly found to be 5-3-4 (number of neurons in input layer, 5; number of neurons in hidden layer, 3; and number of neurons in output layer, 4); i.e., this architecture yielded the maximum accuracy on the test sets. The accuracy of ANN on the basis of jack knife validation is 94.9%.

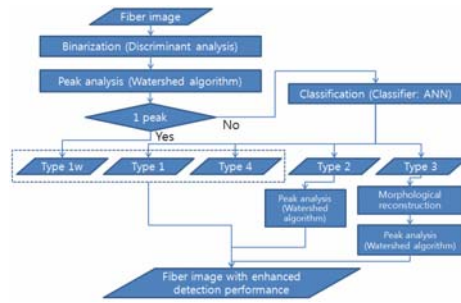


Figure 2: Flow chart of enhanced algorithm

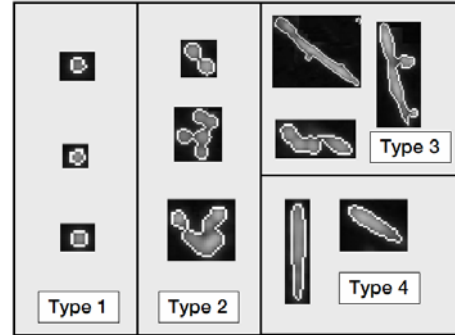


Figure 3: Typical fiber image

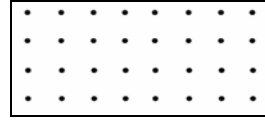
Test result and discussion

Fig. 4 shows artificial fiber images and the α_f values calculated by the suggested algorithm. This demonstrates correct calculations, showing α_f values of 1.0 and 0.041 for the images with perfect dispersion (Fig. 4(a)) and with severely biased dispersion (Fig. 4(b)). Fig. 5 shows the fluorescence image tested in order to assess the detection performance of the enhanced algorithm. Fig. 5 displays the detection test results, where the white point located on the grayscale image (fiber) indicates the center of the detected fiber image. A, B, and C fiber images in Fig. 5, which were classified as Type 2 fibers, were more successfully detected using the enhanced algorithm relative to the results of the proto-type algorithm (Fig. 6). Detection results of C, D, and E fiber image (Type 3) in Fig. 6 are also indicative of significantly improved fiber-detection performance minimizing over-segmentation of the enhanced algorithm. All results in Fig. 6(c) indicate that the enhanced algorithm yields significantly improved fiber-detection performance.

Table 1 compares α_f values calculated by the proto-type algorithm and the enhanced algorithm. As shown in Table 1, the enhanced algorithm provides lower α_f values, i.e. increased by 9.36%, compared to the proto-type algorithm. This is most likely due to correct segmentation of the fibers from the aggregate fiber images, where the fibers are located close enough to decrease the average α_f for the same sample. On the other hand, the enhanced algorithm minimizing over-segmentation provides higher α_f values, i.e. decreased by 2.39%, compared to the enhanced algorithm without considering over-segmentation. This is most likely due to correct segmentation of the fibers from Type 3 fiber images.

Table 1: α_f values calculated by proto-type and enhanced algorithms

	Proto-type algorithm	Enhanced algorithm (over-segmentation)	Enhanced algorithm
α_f	0.3836	0.3396	0.3477



(a) perfect dispersion



(b) severely biased dispersion

Figure 4: Artificial fiber images to test

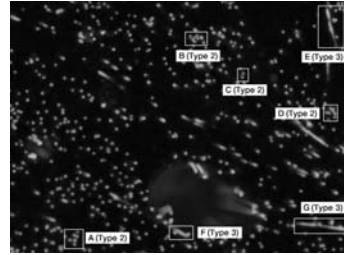
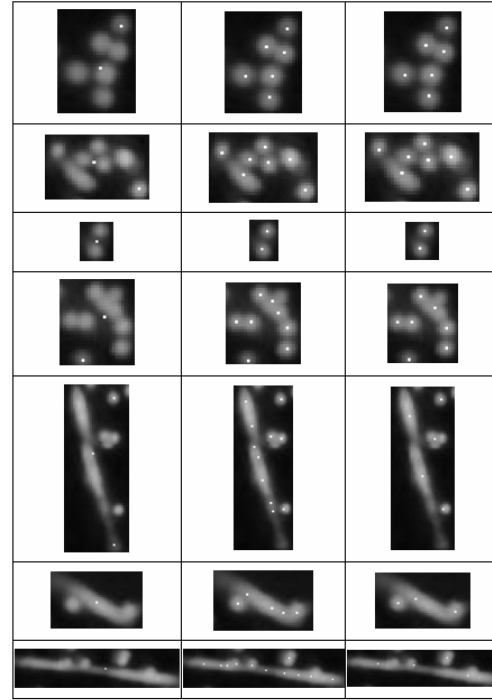


Figure 5: Test image



(a) proto-type algorithm (b) enhanced algorithm (over-segmentation) (c) enhanced algorithm

Figure 6: Test results (the white point indicates each fiber)

Conclusion

This paper proposes a new procedure to evaluate PVA fiber dispersion in a cementitious composite. A series of experimental and analytical investigations was carried out to verify the validity of this procedure. The following conclusions can be drawn from the current results: (1) This procedure is essentially composed of four tasks: Task 1, preparation and treatment of the specimen; Task 2, acquisition of a fluorescence image; Task 3, automatic detection of fibers in a binary image originally converted from the fluorescence image; and Task 4, mathematical treatment of the data obtained from the previous step. In the third step, Task 3, a fiber categorizing technique and morphological reconstruction of fiber images and watershed segmentation technique were employed to enhance the fiber-detection accuracy; (2) The fiber images detected by the proto-type algorithm were classified into five types. In this study, to classify the fiber images, an ANN was constructed. Five-type categorization was carried out to enhance fiber-detection by deliberately selecting incorrectly detected fiber images (Type 2 and Type 3) separately from cor-

rectly detected images (Type 1 and Type 4) by the proto-type algorithm. For this process, features which are used as inputs of a classifier are extracted. In addition, to correctly detect aggregate fiber images (Type 2 and Type 3), the watershed algorithm and morphological reconstruction were used. Based on an experiment, the fiber-detection performance was found to be improved by the enhanced algorithm.

Acknowledgement

This study has been a part of a research project supported by the Ministry of Construction and Transportation(MOCT) of the Korean government via the Infra-Structures Assessment Research Center.

References

1. Li, V. C., Wang, S. and Wu, C. (2001): "Tensile strain-hardening behavior of polyvinyl alcohol-engineered cementitious composite (PVA-ECC)", *ACI Materials Journal*, Vol. 98, No. 6, pp. 483-492.
2. Li, V. C. (2002), "Reflections on the research and development of ECC", *Proceedings of the JCI Int'l Workshop on Ductile Fiber Reinforced Cementitious Composites Application and Evaluation (DFRCC'2002)*, Takayama, Japan, Oct., 1-21.
3. Kim, Y. Y., Kong, H-J and Li, V. C. (2003): "Design of engineered cementitious composite suitable for wet-mixture shotcreting", *ACI Materials Journal*, Vol. 100, No. 6, pp. 511-518.
4. Torigoe, S., Horikoshi, T., and Ogawa, A. (2003): "Study on evaluation method for PVA fiber distribution in engineered cementitious composite", *Journal of Advanced Concrete Technology*, Vol. 1, No. 3, pp. 265-268.
5. Kobayashi, K. (1981): "Fiber reinforced concrete", Tokyo: Ohm-sha.
6. Otsu, N. A. (1979): "Threshold Selection Method from Gray Level Histogram", *IEEE Transactions on Systems, Man, and Cybernetics*, SMC-9(1), pp. 62-66.
7. Krogh, A., Hertz, J. A. (1992): A simple weight decay can improve generalization. In: Moody JE, Hanson SJ, Lippmann RP, editors. *Advances in Neural Information Processing Systems 4*. Morgan Kaufmann Publishers, pp. 950-957.